

Genetic and pharmacological inhibition of JNK ameliorates hypoxia-induced retinopathy through interference with VEGF expression

Monica Guma^{a,b,c,1}, Jordi Rius^{a,b,c,1}, Karen X. Duong-Polk^d, Gabriel G. Haddad^e, James D. Lindsey^d, and Michael Karin^{a,b,c,2}

^aLaboratory of Gene Regulation and Signal Transduction, Departments of ^bPharmacology, ^cPathology, and ^ePediatrics, School of Medicine, and ^dHamilton Glaucoma Center, University of California at San Diego, 9500 Gilman Drive, La Jolla, CA 92093-0723

Contributed by Michael Karin, March 10, 2009 (sent for review January 15, 2009)

Many ocular pathologies, including retinopathy of prematurity (ROP), diabetic retinopathy, and age-related macular degeneration, result in vision loss because of aberrant neoangiogenesis. A common feature of these conditions is the presence of hypoxic areas and overexpression of the proangiogenic vascular endothelial growth factor (VEGF). The prevailing current treatment, laser ablation of the retina, is destructive and only partially effective. Preventive and less destructive therapies are much more desirable. Here, we show that mice lacking c-Jun N-terminal kinase 1 (JNK1) exhibit reduced pathological angiogenesis and lower levels of retinal VEGF production in a murine model of ROP. We found that hypoxia induces JNK activation and regulates VEGF expression by enhancing the binding of phospho-c-Jun to the VEGF promoter. Intravitreal injection of a specific JNK inhibitor decreases retinal VEGF expression and reduces pathological retinal neovascularization without obvious side effects. These results strongly suggest that JNK1 plays a key role in retinal neoangiogenesis and that it represents a new pharmacological target for treatment of diseases where excessive neoangiogenesis is the underlying pathology.

neoangiogenesis | retinopathy of prematurity

Retinopathy of prematurity (ROP) is the leading cause of childhood blindness in industrialized countries and affects premature infants exposed to high oxygen concentrations (1, 2). As in other ocular pathologies, such as diabetic retinopathy and age-related macular degeneration (AMD), vision loss is the result of aberrant neoangiogenesis caused by overexpression of the proangiogenic factor VEGF (3–5). ROP is a biphasic disease consisting of an initial phase of hyperoxia that induces irreversible damage to immature retinal vessels of the neonate, resulting in retinal ischemia, followed by a second phase of hypoxia-induced pathological neoangiogenesis. This retinopathy usually regresses but can lead to irreversible vision loss if there is progression from retinal neovascularization to cicatrization and retinal detachment (1, 2).

VEGF is an essential cytokine in hypoxia-induced proliferative retinopathy (6, 7). In the first phase of ROP, supplemental oxygen suppresses VEGF production, thereby interfering with normal vascular development. In the second phase, which follows oxygen-induced vessel loss and subsequent hypoxia, retinal VEGF expression is induced, resulting in pathological neovascularization. Intravitreal injection of VEGF inhibitors during this phase decreases the neovascular response, indicating that VEGF is a critical factor contributing to retinal vascularization (3, 8). Excessive VEGF production and aberrant neoangiogenesis have also been implicated in retinal neovascularization in diabetic retinopathy (9) and choroidal neovascularization in AMD (10).

The Jun kinases (JNK) belong to the mitogen-activated protein kinase (MAPK) family (11). These kinases, which are encoded by three separate loci, *Jnk1-3*, regulate key cellular processes such as cell proliferation, migration, survival, and cytokine production. In cell culture studies, a nonspecific JNK inhibitor was shown to affect VEGF mRNA stabilization (12). However, the in vivo role of JNK1

in control of VEGF production and angiogenesis has not been investigated.

In this report, we show that JNK1 is a critical factor in hypoxia-induced retinal VEGF production and that it promotes hypoxia-induced pathological angiogenesis. JNK1 deficiency or JNK inhibition results in reduced pathological angiogenesis and lower levels of retinal VEGF in an experimental model of ROP. We also found that JNK1 regulates VEGF expression at the transcriptional level through Jun protein phosphorylation. Our results strongly suggest that JNK1 plays a key role in the development of ROP and that JNK inhibition may be an effective way to treat this disease.

Results

JNK1 Regulates VEGF Expression and Neovascularization in a Murine Model of Retinopathy. To determine whether regulation of VEGF production is a general pathophysiological function of JNK1, we analyzed its role in oxygen-induced retinopathy (OIR), a well-established model of ROP (13). In this model, when mouse pups are exposed to hyperoxia (75% oxygen) from postnatal day 7 to postnatal day 12 (from P7 to P12), vessel regression and cessation of normal radial vessel growth occur, thus mimicking the first phase of ROP. Upon return to ambient air (normoxia) from P12 to P17, the nonperfused regions of the retina become hypoxic, resulting in expression of angiogenic factors, such as VEGF, and retinal neovascularization. The neovascular phase in this model is similar to the second phase of ROP in humans and, in addition, mimics certain aspects of proliferative diabetic retinopathy. Thus, we used retinas from P17 animals to assess the maximum neovascular response.

We found that the absence of JNK1 had a protective effect against pathological angiogenesis. In mice subjected to the OIR model, flat-mounted retinas that were stained with isolectin G4 from *Griffonia simplicifolia*, a specific marker of endothelial cells, and quantified as explained in *Methods*, JNK1-deficient mice had a similar vasoobliterated/total retina area of $8.2 \pm 3.4\%$ vs. $9.2 \pm 1.1\%$ (an insignificant difference) at P17. However, pathological neovascularization was significantly reduced in retinas of *Jnk1*^{-/-} mice ($18.4 \pm 2.8\%$ vs. $11.7 \pm 2.6\%$ neovascularization, $P = 0.01$; Fig. 1 *A* and *B*). Because this model is a well-characterized VEGF-dependent model (7, 14, 15) and suppression of VEGF expression or activity inhibits neovascularization in several diseases (3, 4), we examined whether the absence of JNK1 reduces VEGF expression. ELISA of total retinal protein extracts from OIR mice at P17 showed a significant reduction in the amount of retinal VEGF in *Jnk1*^{-/-} mice relative to *wild-type* (WT) counterparts (Fig.

Author contributions: M.G., J.R., G.G.H., J.D.L., and M.K. designed research; M.G., J.R., and K.X.D.-P. performed research; M.G., J.R., and M.K. analyzed data; and M.G., J.R., and M.K. wrote the paper.

The authors declare no conflict of interest.

¹M.G. and J.R. contributed equally to this work.

²To whom correspondence should be addressed. E-mail: mkarin@ucsd.edu.

This article contains supporting information online at www.pnas.org/cgi/content/full/0902659106/DCSupplemental.

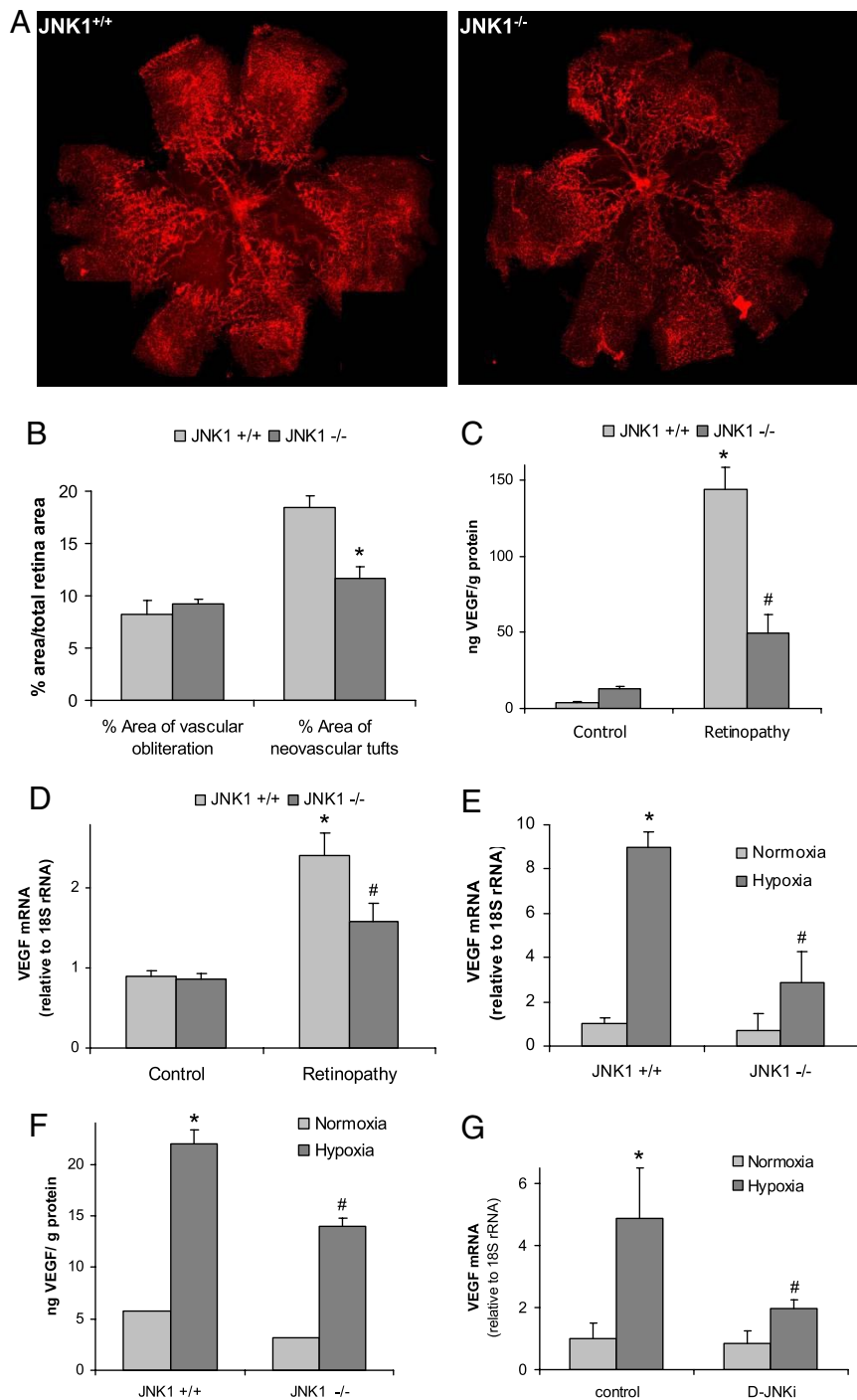


Fig. 1. JNK1 regulates VEGF expression and neovascularization in a murine model of retinopathy. Litters of *Jnk1*^{+/+} and *Jnk1*^{-/-} pups with at least two nursing dams per group were placed under hyperoxia (75% oxygen) or ambient air for 5 days on P7. After 5 days, on P12, mice were returned to ambient air until P17, when they were killed; their eyes were enucleated, and retinas were isolated. (A) Whole-mounted retinas from mice exposed to hyperoxia followed by normoxia were stained with Alexa Fluor 594-conjugated B4 isolectin from *G. simplicifolia* and viewed by fluorescent microscopy. (B) Areas of vascular obliteration and neovascular tufts were quantified by using at least 6 mice per genotype. Results are expressed as means \pm SEM. *, $P < 0.05$ vs. WT mice. (C) Retinal proteins were extracted at P17, and VEGF was quantified by ELISA. Results are averages of two experiments using at least 6 mice per genotype. Results are expressed as means \pm SEM. *, $P < 0.05$ vs. control; #, $P < 0.05$ vs. WT mice. (D) Retinal RNA was extracted at P15, and VEGF mRNA was analyzed by Q-RT-PCR ($n = 4$ per genotype). Results are expressed as means \pm SEM. *, $P < 0.05$ vs. control; #, $P < 0.05$ vs. WT mice. (E) BMDM from either *Jnk1*^{+/+} or *Jnk1*^{-/-} mice were exposed to normoxia ($P_{O_2} = 21\%$) or hypoxia ($P_{O_2} = 0.5\%$) for 4 h. RNA was extracted, and VEGF mRNA was quantified by Q-RT-PCR. Results are expressed as means \pm SEM. *, $P < 0.05$ vs. normoxic *Jnk1*^{+/+} BMDM; #, $P < 0.05$ vs. hypoxic *Jnk1*^{+/+} BMDM. (F) BMDM were treated as above, and VEGF protein expression was analyzed by ELISA. Results are expressed as means \pm SEM. *, $P < 0.05$ vs. normoxic *Jnk1*^{+/+} BMDM; #, $P < 0.05$ vs. hypoxic *Jnk1*^{+/+} BMDM. (G) U87 cells were preincubated (1 h) with D-JNKi (1 μ M) and cultured under normoxia ($O_2 = 21\%$) or hypoxia ($O_2 = 0.5\%$) for 4 h. RNA was extracted, and VEGF expression was analyzed by Q-RT-PCR. Results are expressed as means \pm SEM. *, $P < 0.05$ vs. normoxic control cells; #, $P < 0.05$ vs. hypoxic control cells.

1C). To assess whether JNK1 controls VEGF expression transcriptionally, we isolated RNA from retinas with induced neovascularization at P15 and measured VEGF mRNA amounts. Induction of VEGF mRNA was significantly reduced in *Jnk1*^{-/-} mice (Fig. 1D). No substantial differences between *Jnk1*^{-/-} and WT mice were found for other mRNAs, including those encoding hypoxia-regulated proteins or inflammatory factors that are involved in OIR, such as tumor necrosis factor α (TNF- α ; 16) [supporting information (SI) Fig. S1].

After P12, the nonperfused regions of the retina become hypoxic, and because JNK1 deficiency is known to prevent ischemic cell death (17, 18), we examined the retinas of P14 animals for the presence of cells undergoing apoptosis. There were no differences

between *Jnk1*^{-/-} and WT mice as assayed by in situ terminal deoxynucleotidyl transferase-mediated dUTP nick-end labeling (TUNEL; Fig. S2).

Glia-derived cells such as astrocytes present in the ganglion cell layer, Muller cells embedded in the inner nuclear layer (14, 15), and macrophages recruited into the retina were described as major sources of retinal VEGF in ROP (19, 20). Although retinal pigmented epithelium residing at the outer boundary of the neural retina was suggested as another source of retinal VEGF, expression of VEGF mRNA by these cells was shown to be unaffected in this model (7, 15). Because of the scarcity and the difficulty in isolation of the different VEGF-producing cell types from mouse retinas, we used a variety of other JNK1-deficient cell types to characterize

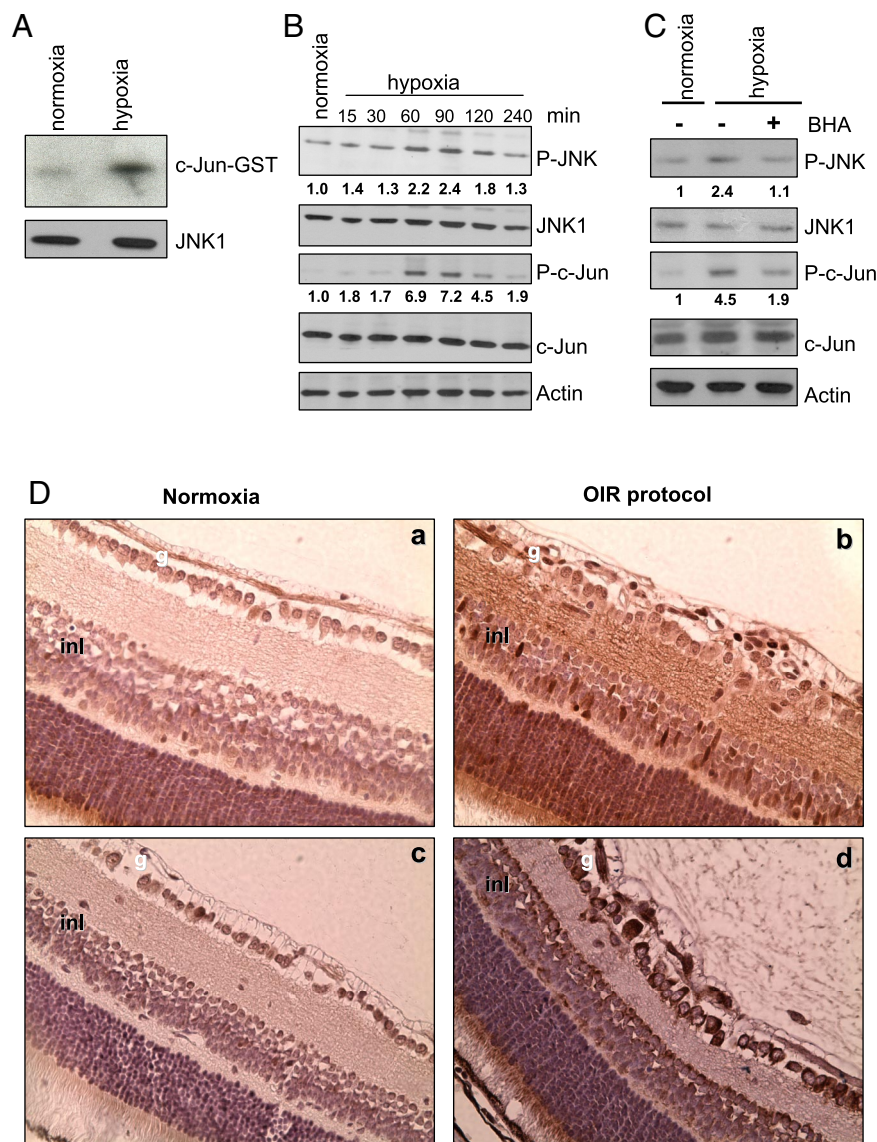


Fig. 2. Hypoxia induces JNK activation. RAW264.7 macrophages were cultured either normoxia ($P_{O_2} = 21\%$) or hypoxia ($P_{O_2} = 0.5\%$). (A) Cell lysates were obtained after 1 h under normoxia or hypoxia, and JNK activity was measured by immunocomplex kinase assay using GST-c-Jun (1–79) as a substrate. (B) Amounts of phosphorylated (P) JNK and c-Jun were analyzed by immunoblotting at different times after initiation of hypoxia. Numbers below P-JNK and P-c-Jun blots represent relative values normalized to total JNK and c-Jun amounts. (C) Cells were preincubated without or with BHA ($10 \mu\text{M}$) for 1 h, cultured under normoxia or hypoxia for 1 h, and analyzed as in B. (D) Retinas from P15 mice either under normoxia or subjected to OIR were stained with antibodies to phospho-c-Jun (a and b) or VEGF (c and d). g, ganglionar cell layer; inl, inner nuclear layer.

further the role of JNK1 in hypoxia-induced VEGF production. Hypoxia-induced VEGF mRNA and protein were substantially lower in *Jnk1*^{-/-} bone marrow-derived macrophages (BMDM) and murine embryonic fibroblasts (MEFs) relative to WT counterparts (Fig. 1 E and F and Fig. S3). In U87 glioma cells the hypoxic induction of VEGF mRNA was reduced upon treatment with a highly specific and cell-permeable JNK peptide inhibitor, D-JNKi (Fig. 1G), which has been successfully used by several groups for treatment of JNK-mediated pathologies (21–23).

Hypoxia Induces JNK Activation. We addressed the mechanism of JNK1-dependent VEGF expression. As described (24, 25), hypoxia enhanced JNK kinase activity (Fig. 2A) and the phosphorylation of JNK and c-Jun, an established JNK substrate (Fig. 2B). Hypoxia results in accumulation of reactive oxygen species [ROS (26)], and ROS can lead to JNK activation through several mechanisms, including the oxidation and inhibition of MAPK phosphatases (27). Correspondingly, treatment of hypoxic cells with butylated hydroxyanisole (BHA), a potent antioxidant, decreased both JNK and c-Jun phosphorylation (Fig. 2C). Using immunohistochemistry, we found that at P15 c-Jun phosphorylation was increased in nearly all layers of the retina in OIR mice (Fig. 2D). Intense c-Jun phosphor-

ylation was detected in both the ganglionar and inner nuclear layers, where cells responsible for VEGF production reside.

JNK1 Does Not Regulate HIF-1 α Expression. Hypoxia-inducible factor-1 α (HIF-1 α) is a well-studied mediator of the cellular response to low oxygen and plays a major role in hypoxia-induced transcriptional activation of VEGF (28, 29). We recently found that in addition to its hypoxia-induced stabilization (30), HIF-1 α expression is also transcriptionally regulated by NF- κ B (31). However, JNK1 deficiency did not interfere with the hypoxic induction of HIF-1 α (Fig. 3A) or HIF-1 α target genes, other than VEGF (Fig. 3B).

JNK1 Regulates VEGF Transcriptional Activity. In addition to an HIF-1 α -binding site, the VEGF promoter contains multiple AP-1 transcription factor-binding sites, and the AP-1 site at position -1093 to -1086 was shown to be critical for hypoxia-induced transcription (32). Consistent with these results, we found that hypoxia-induced VEGF promoter activity was reduced when this AP-1 site or the hypoxia response element (HRE) was inactivated (Fig. 4A). Treatment of cells with D-JNKi reduced VEGF promoter activity to the same extent as did ablation of the AP-1 site, suggesting that AP-1 activity at the VEGF promoter is regulated via the JNK pathway.

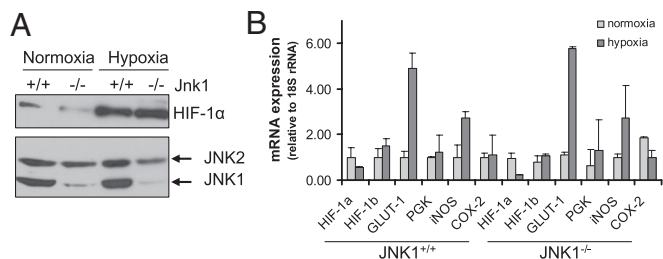


Fig. 3. JNK1 does not regulate HIF-1 α expression. BMDM from either WT or *Jnk1*^{-/-} mice were cultured under normoxia (Po₂ = 21%) or hypoxia (Po₂ = 0.5%) for 4 h. (A) Cells were harvested, and cytosolic and nuclear extracts were prepared. Protein expression of JNK1/2 (cytosolic) and HIF-1 α (nuclear) was examined by immunoblotting. (B) RNA was extracted and quantified by Q-RT-PCR. Results of three separate experiments done in triplicate are expressed as means \pm SEM.

It was suggested that hypoxia-induced JunB transcription is involved in VEGF expression (33). However, we did not observe any difference in JunB amounts between JNK1-deficient and WT cells (Fig. S4). c-Jun is a better JNK substrate than JunB (34) and can form homo- and heterodimers that bind to AP-1 sites (11, 35). Hypoxia induced c-Jun phosphorylation at serine (S) 63, a rate-limiting step in c-Jun-mediated transactivation (36), in a JNK1-dependent manner (Fig. 4B). Using chromatin immunoprecipitation (ChIP) we found that hypoxia increases the amount of phospho-S63-c-Jun bound to the VEGF promoter (Fig. 4C). These data show that hypoxia can induce VEGF transcription through activation of the JNK1-c-Jun pathway in addition to the well-established HIF-1 pathway.

Intravitreal Injection of a JNK Inhibitor Prevents Retinal Neovascularization. The results shown above suggest that JNK1 is an excellent target for treating ROP because its inhibition can reduce vascular overgrowth without completely abolishing VEGF expression. This fact can be very important in ROP treatment because VEGF is a

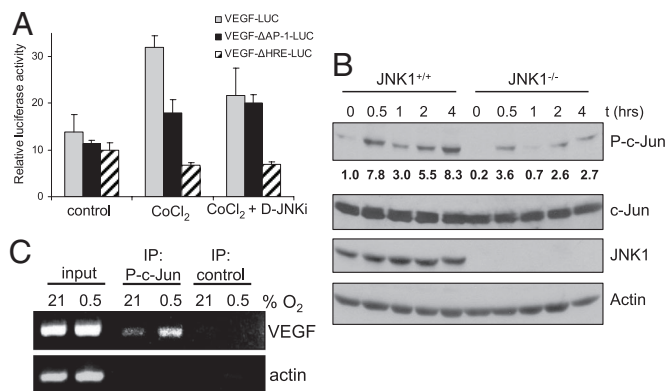


Fig. 4. JNK1 regulates VEGF transcriptional activity. (A) RAW264.7 macrophages were transfected with pVEGF-Luc, pVEGF Δ AP-1-Luc, or pVEGF Δ HRE-Luc reporters. After 24 h, cells were treated with the hypoxia mimetic CoCl₂ (200 μ M). Some of the cells were pretreated with D-JNKi (1 μ M) for 1 h. Results represent mean \pm SEM luciferase activity relative to the internal control pRL-TK, in three separate experiments performed in triplicate. (B) *Jnk1*^{+/+} and *Jnk1*^{-/-} BMDM were cultured under normoxia (Po₂ = 21%) or hypoxia (Po₂ = 0.5%). At different time points, cell lysates were prepared and analyzed for phosphorylated (P) or total amounts of the indicated proteins by immunoblotting. Numbers below P-c-Jun blot represent relative values normalized to total c-Jun. (C) ChIP was performed with anti-phospho-S63-c-Jun or a control antibody by using fixed and sheared chromatin isolated from RAW264.7 mouse macrophages cultured under normoxia or hypoxia for 1 h. The VEGF promoter fragment, which contains an AP-1 site at -1093/-1086 bp, was detected by PCR. The actin promoter served as a control.

key survival factor for neurons (37). To examine the ability of a JNK inhibitor to treat ROP, we tested whether D-JNKi injected intravitreally once on day 14 could prevent neovascularization in the OIR model. We also examined whether D-JNKi can inhibit retinal c-Jun phosphorylation in OIR mouse pups. At P15, phosphorylated c-Jun was evident in the retina of untreated OIR mice, but c-Jun phosphorylation was decreased in D-JNKi-treated retinas (Fig. 5A). Inhibition of retinal neovascularization by D-JNKi was clearly evident in flat-mounted retinas analyzed at P17, showing a reduction of neovascular tufts, despite comparable pericentral avascular zones (21.5 \pm 6.4% vs. 13.2 \pm 7.3% neovascularization, P < 0.05) (Fig. 5B and C). D-JNKi treatment also reduced the amount of retinal VEGF (Fig. 5D).

Importantly, D-JNKi treatment had no visible side effects as judged by histological examination of the retinas. In addition, the treatment had no effect on the number of ganglion cells, width of the whole retina, and width of the inner and outer nuclear layers (Fig. 5E and Table S1). There were also no differences in apoptosis as assayed by TUNEL staining (Fig. S5). Furthermore, retinas of *Jnk1*^{-/-} mice had completely normal appearance under normoxic conditions (Fig. S6). Thus, JNK inhibition reduces abnormal VEGF expression and retinal neovascularization without producing retinal damage or impairing retinal development.

Discussion

In this work, we show that JNK1 is a critical factor in hypoxia-driven pathological angiogenesis in the retina. Mice lacking the *Jnk1* gene or treated with a specific JNK inhibitor peptide show a marked reduction in retinal neovascularization induced by oxygen exposure followed by a period of relative hypoxia, an experimental model of ROP. Currently, ROP is a major complication in oxygen-treated premature newborns and the leading cause of blindness in children in developed countries. Although oxygen therapy improves survival of premature newborns, it also increases oxygen levels in the developing retina, thereby inhibiting VEGF expression and vascular development. Yet, the neural structures of the peripheral avascular retina continue to develop, a situation that results in local hypoxia that eventually increases VEGF production and results in abnormal angiogenesis. The current therapeutic strategies for ROP, which are based on ablation of the avascular retina by using cryotherapy or laser photocoagulation, are moderately successful with several side effects. Thus, it is desirable to identify new and improved therapies. A new popular approach to prevention of abnormal neovascularization is inhibition of VEGF activity. Abnormal expression of VEGF has also been linked to several ocular pathologies such as AMD and diabetic retinopathy, and currently VEGF inhibition is used to treat some forms of AMD.

VEGF production is tightly regulated in vivo, and mice lacking only one copy of the *Vegf* gene exhibit embryonic lethality resulting from abnormal blood vessel development (38, 39). Thus, inhibition of VEGF expression needs to be approached carefully in neonates to avoid systemic complications caused by incomplete angiogenesis. One way to avoid long-lasting inhibition of VEGF is to inhibit VEGF expression rather than sequester the protein with a neutralizing antibody. The main factors that control VEGF expression in response to hypoxia are HIF-1 and HIF-2 (28, 40, 41). Although siRNA targeting of HIF-1 α was found to decrease neovascularization in the OIR model (42), so far there are no specific pharmacological inhibitors that prevent HIF-1 activation.

We now show that another important factor involved in VEGF induction is JNK1. JNK family members are involved in cell proliferation, apoptosis, and cytokine production (11). Yet, the in vivo role of JNK in hypoxia-induced VEGF production and the feasibility of using JNK as a target to control aberrant angiogenesis have not been evaluated. We found that JNK1 is critical for hypoxia-induced retinal VEGF production and pathological ocular angiogenesis. Retinal JNK-dependent VEGF expression occurs independently of HIF activation, and hypoxia stimulates JNK

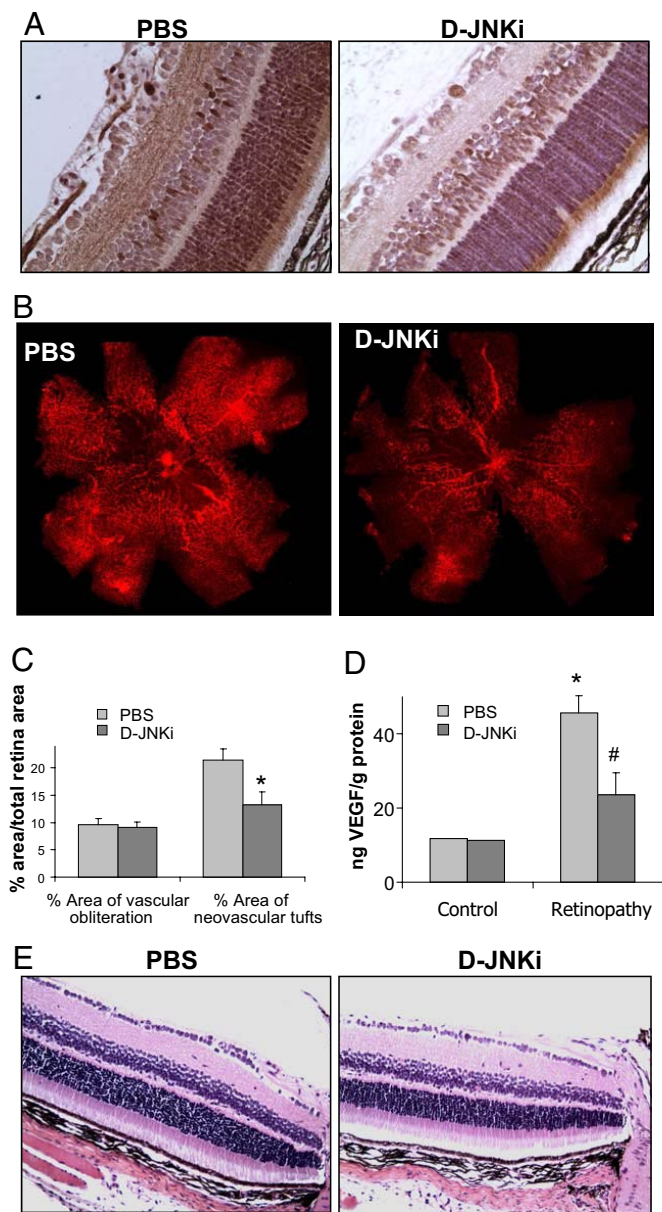


Fig. 5. Intravitreal injection of a JNK inhibitor prevents retinal neovascularization. Mice subjected to OIR were injected intravitreally once with either PBS or D-JNKi at P14. (A) c-Jun phosphorylation was examined by immunohistochemistry at P15. (B) On P17, mice were killed, and their eyes were enucleated, and retinas were isolated and stained as in Fig. 1. (C) Areas of vascular obliteration and neovascular tufts were quantified as in Fig. 1A ($n = 10$ per genotype). Results are expressed as means \pm SEM. *, $P < 0.05$ vs. WT mice. (D) Protein was extracted from retinas at P17, and VEGF concentration was measured by ELISA ($n = 8$ per genotype). Results are expressed as means \pm SEM. *, $P < 0.05$ vs. control; #, $P < 0.05$ vs. WT mice. (E) Mice injected at P18 with PBS or D-JNKi were assessed at P28 by staining retinal cross-sections with hematoxylin and eosin under normoxic conditions.

activity through ROS production. Once activated, JNK induces c-Jun phosphorylation at the VEGF promoter. Consequently, genetic ablation of JNK1 or pharmacological interference with JNK activity reduces vascular overgrowth without completely abolishing VEGF expression. This could be important because VEGF is a key neurotrophic factor (37). Although some studies have shown that neutralizing anti-VEGF antibodies do not cause retinal toxicity (43), it was also observed that such treatments can induce mitochondrial disruption in inner photoreceptor segments (44).

Moreover, it was recently reported that high intravitreal doses of an anti-VEGF antibody can increase the risk of stroke (45). By contrast, JNK inhibitors have been proposed to prevent cell death associated with stroke and myocardial infarction (21, 46). It is also likely that JNK inhibition may prevent ischemia-induced edema, which has also been linked to abnormal VEGF production (47).

In summary, our work shows that JNK1 is a critical factor in hypoxia-induced retinal VEGF production and pathological angiogenesis. JNK1 deficiency or JNK inhibition does not alter normal retinal development and does not impact retinal anatomy, a crucial point for drugs that are used in neonates. JNK inhibition can attenuate the development of ROP and may be an effective treatment for this disease.

Methods

Mouse Model of OIR. OIR was induced as described in ref. 13. Briefly, 7-day-old (P7) WT and *Jnk1*^{-/-} mouse pups (C57BL/6J background) were exposed to 75% O₂ for 5 days with nursing mothers, by using an incubator in which O₂ tension was controlled by the Oxycycler hydraulic system (model A44x; BioSpherix) and ANA-Win2 Software (Version 2.4.17; Watlow Anafaze). The mice were placed in the O₂ incubator with enough food and water to sustain them for 5 days, from P7 to P12. At P12, the animals were returned to room air for 5 days until P17, when their retinas were assessed for maximum neovascular response. Control mice were kept in the same room under ambient O₂ and were exposed to the same level of noise and light for the duration of each experiment. All animals were housed in Association for Assessment and Accreditation of Laboratory Animal Care-approved vivaria in the School of Medicine, University of California San Diego, following standards and procedures approved by the local Institutional Animal Care and Use Committee for the ethical use of laboratory animals.

Quantification of Vasoobliteration and Retinal Neovascularization. Mice were killed on P17 and perfused via the left ventricle with 4% paraformaldehyde. Eyes were enucleated and fixed for 2 h in 4% paraformaldehyde. Retinas were dissected and then soaked in methanol for 15 min on ice, followed by blocking (BioGenex) for 2 h. Retinas were stained overnight in Alexa Fluor 594-conjugated *G. simplicifolia* isolectin B4 (I-21413, 1:100 dilution; Molecular Probes). Imaging quantification was described in ref. 48. Briefly, retinal flat mounts were generated and images were taken at 5x magnification. Between 4 and 8 overlapping images were acquired from each retina. No image manipulation was performed in terms of background, intensity, or color curves. Retinal images were imported into Adobe Photoshop (Photoshop 6.0; Adobe Systems) and merged to produce an image of the whole retina. Subsequent quantification was performed on these montages by using image analysis software (MiraMon 6.2; Geographic Information System and Remote Sensing software; Autonomous University of Barcelona). Both area of obliteration and areas of neovascular tufts in pixels were related to the total retinal area in pixels and given as percentages.

Intravitreal Injection. Intravitreal injections of either PBS or D-JNKi (500 μ M) were conducted either at P14 of the OIR model or at P18 under normoxic conditions. At P14 of the OIR model, D-JNKi was injected only once and, retinas were assessed at P15 for anti-phospho-S63-c-Jun staining and at P17 for VEGF production and vessel quantification. At P18 under normoxic conditions, D-JNKi was also injected once, and retinas were assessed at P19 for TUNEL staining and at P28 for evaluation of acute tissue toxicity. A microglass needle with a bevelled tip 60–100 μ m in diameter was connected to a 25- μ L luer tip fitting Hamilton microsyringe. Microinjection was done by mounting the microsyringe on a Micro4 MicroSyringe pump controller attached to a micromanipulator (WPI). A total volume of 1 μ L was infused into the vitreous of the right eye at a rate of 50 nL/s.

Reagents. The D-JNKi peptide composed of D amino acids DQSRPVQFPLNLT-TPRKPRPPRRRQRKKRG, was synthesized by the Protein Chemistry Department at the Research Institute of Molecular Pathology and was provided by Erwin Wagner (Institute of Molecular Pathology, Vienna). Specific inhibition of JNK by D-JNKi is shown in ref. 21. BHA was purchased from Sigma. Cells were preincubated without or with BHA (10 μ M) for 1 h and cultured under normoxia or hypoxia for 1 h.

ELISA. Retinas were homogenized in lysis solution. Protein concentration was measured, and VEGF ELISA was performed according to the manufacturer's instructions (R&D Systems).

Quantitative (Q)-RT-PCR. RNA was extracted with TRIzol (Invitrogen) and reverse transcribed with a SuperScript II kit (Invitrogen). Q-PCR was performed with SYBR

Green PCR Master Mix (Applied Biosystems). Primer sequences are available upon request.

Kinase Assay. Cells were lysed and immunoprecipitated with an anti-JNK1 antibody (BD Biosciences). The immunocomplexes were incubated with GST-c-Jun(1–79) in the presence of [γ - 32 P]ATP. Proteins were resolved by SDS/PAGE and transferred to a nitrocellulose membrane that was exposed to X-ray film and hybridized with an anti-JNK1 antibody (Santa Cruz Biotechnology) to normalize for protein loading.

Histology and TUNEL Assay. The eyes were enucleated and fixed in 4% paraformaldehyde overnight before embedding in paraffin. Serial 5- μ m paraffin-embedded axial sections were obtained from the optic nerve and stained with hematoxylin and eosin, and images were taken at 20 \times magnification. Layer widths (mm) were measured at 2 and at 4 cm from optic nerve, in both the upper and lower sides of the retina. We also counted ganglion cells between the optic nerve and 4 cm from that point. Results are averages \pm SD. For immunohistochemistry, sections were incubated overnight at 4 $^{\circ}$ C with anti-phospho-S63-c-Jun (Cell Signaling) or anti-VEGF (sc-507; Santa Cruz Biotechnology) at a 1:50 dilution. In situ TUNEL assay was performed by using ApoAlert DNA fragmentation assay kit (Clontech).

Immunoblotting. Whole-cell extracts were obtained by lysing cells in 1% SDS, 10 mM Tris-HCl (pH 7.4). Proteins were separated by SDS/PAGE and transferred to a membrane that was incubated with antibodies against phosphorylated JNK (Cell Signaling), JNK1 and JNK1/2 (BD Biosciences), phosphorylated c-Jun, c-Jun, and JunB (Santa Cruz Biotechnology), actin (Sigma), or HIF-1 α (Novus). Immunoblots were quantified by using Quanty one 4.6.5 (Bio-Rad).

ChIP. ChIP was performed by using a ChIP-IT express kit (active motif) according to the manufacturer's instructions. Formaldehyde fixed and sonicated chromatin was precipitated with phospho-S63-c-Jun antibody (Cell Signaling). After reversal

of cross-links and DNA extraction, samples were analyzed by PCR. The murine VEGF and actin promoters were amplified with the primer pairs 5'-GCAGCTG-GCCTACCTACTT-3' and 5'-GACCTGTGGAAACCCACGTA-3' and 5'-TGCACTGT-GCGGCAAGC-3' and 5'-TCGAGCCATAAAAGCAA-3', respectively.

Luciferase Assay. A murine VEGF promoter-luciferase reporter, pVEGF-Luc, and its mutants pVEGF Δ AP-1-Luc and pVEGF Δ HRE-Luc, were kindly provided by Samuel J. Leibovich from New Jersey Medical School (Newark, NJ). Plasmids were cotransfected with internal control, pRL-TK, into Raw-264.7 macrophages by using Lipofectamine 2000 (Invitrogen). After 24 h, cells were treated with 200 μ M CoCl $_2$ for 24 h. D-JNKi inhibitor was used at 1 μ M and added 1 h before the CoCl $_2$ treatment. Luciferase activity was measured by using the Dual-luciferase reporter assay system (Promega). Results are presented as relative reporter activity after normalization to the internal control.

Statistical Analysis. The Kolmogorov–Smirnov nonparametric test was applied to check for normal distribution of continuous variables. To assess the relationship between a categorical variable with two levels and normally or nonnormally distributed quantitative variables, Student's and Mann–Whitney *U* tests were applied, respectively. Multiple groups were compared by one-factor ANOVA, followed by Fisher's protected least-squares difference to assess specific group differences. Analyses were performed with the SPSS 15.0 (SPSS) statistical package. Results were considered significant at the 2-sided *P* level of 0.05.

ACKNOWLEDGMENTS. We thank Dr. Samuel J. Leibovich for providing VEGF promoter-luciferase reporters, Dr. Jonathan H. Lin for examination of tissue histology, and Dr. Randall S. Johnson for the use of his hypoxia chamber. This work was supported by National Institutes of Health grants (to M.K., J.D.L., and G.G.H. laboratories). M.K. is an American Cancer Society Research Professor. J.R. and M.G. were supported by postdoctoral fellowships from the Spanish Ministry of Education and Science. M.G. was also supported by the Spanish Society of Rheumatology.

- Fleck BW, McIntosh N (2008) Pathogenesis of retinopathy of prematurity and possible preventive strategies. *Early Hum Dev* 84:83–88.
- Chen J, Smith LE (2007) Retinopathy of prematurity. *Angiogenesis* 10:133–140.
- Andreoli CM, Miller JW (2007) Anti-vascular endothelial growth factor therapy for ocular neovascular disease. *Curr Opin Ophthalmol* 18:502–508.
- Ferrara N, Kerbel RS (2005) Angiogenesis as a therapeutic target. *Nature* 438:967–974.
- Dorrell M, Uusitalo-Jarvinen H, Aguilar E, Friedlander M (2007) Ocular neovascularization: Basic mechanisms and therapeutic advances. *Surv Ophthalmol* 52(Suppl 1):S3–S19.
- Young TL, et al. (1997) Histopathology and vascular endothelial growth factor in untreated and diode laser-treated retinopathy of prematurity. *J Aapos* 1:105–110.
- Alon T, et al. (1995) Vascular endothelial growth factor acts as a survival factor for newly formed retinal vessels and has implications for retinopathy of prematurity. *Nat Med* 1:1024–1028.
- Kusaka S, et al. (2008) Efficacy of intravitreal injection of bevacizumab for severe retinopathy of prematurity: A pilot study. *Br J Ophthalmol* 92:1450–1455.
- Mason JO, 3rd, Nixon PA, White MF (2006) Intravitreal injection of bevacizumab (Avastin) as adjunctive treatment of proliferative diabetic retinopathy. *Am J Ophthalmol* 142:685–688.
- Takeda AL, Colquitt J, Clegg AJ, Jones J (2007) Pegaptanib and ranibizumab for neovascular age-related macular degeneration: A systematic review. *Br J Ophthalmol* 91:1177–1182.
- Karin M, Gallagher E (2005) From JNK to pay dirt: Jun kinases, their biochemistry, physiology and clinical importance. *JUBMB Life* 57:283–295.
- Pages G, et al. (2000) Stress-activated protein kinases (JNK and p38/HOG) are essential for vascular endothelial growth factor mRNA stability. *J Biol Chem* 275:26484–26491.
- Smith LE, et al. (1994) Oxygen-induced retinopathy in the mouse. *Invest Ophthalmol Visual Sci* 35:101–111.
- Stone J, et al. (1996) Roles of vascular endothelial growth factor and astrocyte degeneration in the genesis of retinopathy of prematurity. *Invest Ophthalmol Visual Sci* 37:290–299.
- Pierce EA, et al. (1995) Vascular endothelial growth factor/vascular permeability factor expression in a mouse model of retinal neovascularization. *Proc Natl Acad Sci USA* 92:905–909.
- Gardiner TA, et al. (2005) Inhibition of tumor necrosis factor- α improves physiological angiogenesis and reduces pathological neovascularization in ischemic retinopathy. *Am J Pathol* 166:637–644.
- Behrens A, Sibilia M, Wagner EF (1999) Amino-terminal phosphorylation of c-Jun regulates stress-induced apoptosis and cellular proliferation. *Nat Genet* 21:326–329.
- Hreniuk D, et al. (2001) Inhibition of c-Jun N-terminal kinase 1, but not c-Jun N-terminal kinase 2, suppresses apoptosis induced by ischemia/reoxygenation in rat cardiac myocytes. *Mol Pharmacol* 59:867–874.
- Naug HL, Browning J, Gole GA, Gobe G (2000) Vitreal macrophages express vascular endothelial growth factor in oxygen-induced retinopathy. *Clin Exp Ophthalmol* 28:48–52.
- Ishibashi T, et al. (1997) Expression of vascular endothelial growth factor in experimental choroidal neovascularization. *Graefes Arch Clin Exp Ophthalmol* 235:159–167.
- Borsello T, et al. (2003) A peptide inhibitor of c-Jun N-terminal kinase protects against excitotoxicity and cerebral ischemia. *Nat Med* 9:1180–1186.
- Kaneto H, et al. (2004) Possible novel therapy for diabetes with cell-permeable JNK-inhibitory peptide. *Nat Med* 10:1128–1132.
- Hui L, et al. (2008) Proliferation of human HCC cells and chemically induced mouse liver cancers requires JNK1-dependent p21 down-regulation. *J Clin Invest* 118:3943–3953.
- Minet E, et al. (2001) c-JUN gene induction and AP-1 activity is regulated by a JNK-dependent pathway in hypoxic HepG2 cells. *Exp Cell Res* 265:114–124.
- Le YJ, Corry PM (1999) Hypoxia-induced bFGF gene expression is mediated through the JNK signal transduction pathway. *Mol Cell Biochem* 202:1–8.
- Chandel NS, et al. (1998) Mitochondrial reactive oxygen species trigger hypoxia-induced transcription. *Proc Natl Acad Sci USA* 95:11715–11720.
- Kamata H, et al. (2005) Reactive oxygen species promote TNF α -induced death and sustained JNK activation by inhibiting MAP kinase phosphatases. *Cell* 120:649–661.
- Forsythe JA, et al. (1996) Activation of vascular endothelial growth factor gene transcription by hypoxia-inducible factor 1. *Mol Cell Biol* 16:4604–4613.
- Oosthuysen B, et al. (2001) Deletion of the hypoxia-response element in the vascular endothelial growth factor promoter causes motor neuron degeneration. *Nat Genet* 28:131–138.
- Kaelin WG, Ratcliffe PJ (2008) Oxygen sensing by metazoans: The central role of the HIF hydroxylase pathway. *Mol Cell* 30:393–402.
- Rius J, et al. (2008) NF- κ B links innate immunity to the hypoxic response through transcriptional regulation of HIF-1 α . *Nature* 453:807–811.
- Pages G, Pouyssegur J (2005) Transcriptional regulation of the vascular endothelial growth factor gene: A concert of activating factors. *Cardiovasc Res* 65:564–573.
- Schmidt D, et al. (2007) Critical role for NF- κ B-induced JunB in VEGF regulation and tumor angiogenesis. *EMBO J* 26:710–719.
- Kallunki T, Deng T, Hibi M, Karin M (1996) c-Jun can recruit JNK to phosphorylate dimerization partners via specific docking interactions. *Cell* 87:929–939.
- Shaulian E, Karin M (2002) AP-1 as a regulator of cell life and death. *Nat Cell Biol* 4:E131–E136.
- Smearl T, et al. (1991) Oncogenic and transcriptional cooperation with Ha-Ras requires phosphorylation of c-Jun on serines 63 and 73. *Nature* 354:494–496.
- Zachary I (2005) Neuroprotective role of vascular endothelial growth factor: Signalling mechanisms, biological function, and therapeutic potential. *Neurosignals* 14:207–221.
- Carmeliet P, et al. (1996) Abnormal blood vessel development and lethality in embryos lacking a single VEGF allele. *Nature* 380:435–439.
- Ferrara N, et al. (1996) Heterozygous embryonic lethality induced by targeted inactivation of the VEGF gene. *Nature* 380:439–442.
- Ema M, et al. (1997) A novel bHLH-PAS factor with close sequence similarity to hypoxia-inducible factor 1 α regulates the VEGF expression and is potentially involved in lung and vascular development. *Proc Natl Acad Sci USA* 94:4273–4278.
- Vinorez SA, et al. (2006) Implication of the hypoxia response element of the Vegf promoter in mouse models of retinal and choroidal neovascularization, but not retinal vascular development. *J Cell Physiol* 206:749–758.
- Jiang J, et al. (2009) Inhibition of retinal neovascularization by gene transfer of small interfering RNA targeting HIF-1 α and VEGF. *J Cell Physiol* 218:66–74.
- Kim JH, et al. (2008) Absence of intravitreal bevacizumab-induced neuronal toxicity in the retina. *Neurotoxicology* 29:1131–1135.
- Inan UU, et al. (2007) Preclinical safety evaluation of intravitreal injection of full-length humanized vascular endothelial growth factor antibody in rabbit eyes. *Invest Ophthalmol Visual Sci* 48:1773–1781.
- Dafer RM, Schneck M, Friberg TR, Jay WM (2007) Intravitreal ranibizumab and bevacizumab: A review of risk. *Semin Ophthalmol* 22:201–204.
- Ferrandi C, et al. (2004) Inhibition of c-Jun N-terminal kinase decreases cardiomyocyte apoptosis and infarct size after myocardial ischemia and reperfusion in anaesthetized rats. *Br J Pharmacol* 142:953–960.
- Weis SM, Chereser DA (2005) Pathophysiological consequences of VEGF-induced vascular permeability. *Nature* 437:497–504.
- Banin E, et al. (2006) T2-TrpRS inhibits preretinal neovascularization and enhances physiological vascular regrowth in OIR as assessed by a new method of quantification. *Invest Ophthalmol Visual Sci* 47:2125–2134.